

# Site-percolation transition of run-and-tumble particles

Soumya K. Saha, Aikya Banerjee, and P. K. Mohanty\*

*Department of Physical Sciences, Indian Institute of Science Education and Research Kolkata, Mohanpur, 741246 India.*

We study percolation transition of run and tumble particles (RTPs) on a two dimensional square lattice. RTPs in these models run to the nearest neighbour along their internal orientation with unit rate, and to other nearest neighbours with rates  $p$ . In addition, they tumble to change their internal orientation with rate  $\omega$ . We show that for small tumble rates, RTP-clusters created by joining occupied nearest neighbours irrespective of their orientation form a phase separated state when the rate of positional diffusion  $p$  crosses a threshold; with further increase of  $p$  the clusters disintegrate and another transition to a mixed phase occurs. The critical exponents of this re-entrant site-percolation transition of RTPs vary continuously along the critical line in the  $\omega$ - $p$  plane, but a scaling function remains invariant. This function is identical to the corresponding universal scaling function of percolation transition observed in the Ising model. We also show that the critical exponents of the underlying motility induced phase separation transition are related to corresponding percolation-critical-exponents by constant multiplicative factors known from the correspondence of magnetic and percolation critical exponents of Ising model.

Active systems consume energy from the environment to produce self-propelled motion [1–6] and lead to nonequilibrium steady states that exhibit collective behavior at many different length scales [6–11]. A specific kind of self-propelled motion performed by certain bacteria and algae [12, 13] are described by a run and tumble dynamics, where particles are assumed to have a sense of direction; they run persistently along their internal orientation and tumble to change their orientation [14–16]. A common phenomenon unique to active matter systems is motility-induced phase separation (MIPS) where the system transit from a mixed to a phase separated state (PSS) with increased motility. It is widely believed that motile particles having only excluded volume repulsion [14, 17–25] can undergo MIPS transition. A stable PSS in the absence of any attractive interaction is surprising and understanding this phenomena has been a center of attention for many researchers in recent years. Active matter systems are modeled theoretically using hydrodynamic descriptions [3, 26, 27] agent based models [28, 29] and lattice models [30–34]. In experiments too, synthetically prepared self-propelled particles [5, 35–38] are found to exhibit collective motion.

In this article, we focus on lattice models of RTPs. In one dimension (1D), RTPs with a constant tumble rate can not phase separate [34]. Models in 2D [39–43] do exhibit phase separation transitions. Characterization of critical behaviour and universality class of MIPS transition is limited, although recent studies [44–47] have claimed the transition to be in Ising universality class. Here, we take a different approach. We study site-percolation properties of RTP-clusters on a square lattice, and deduce the critical behaviour of the underlying MIPS phase transition.

During a percolation transition at least one cluster starts becoming macroscopic in size at the critical point. In a particle conserved system, formation of such a macro-cluster is bound to create a low density region

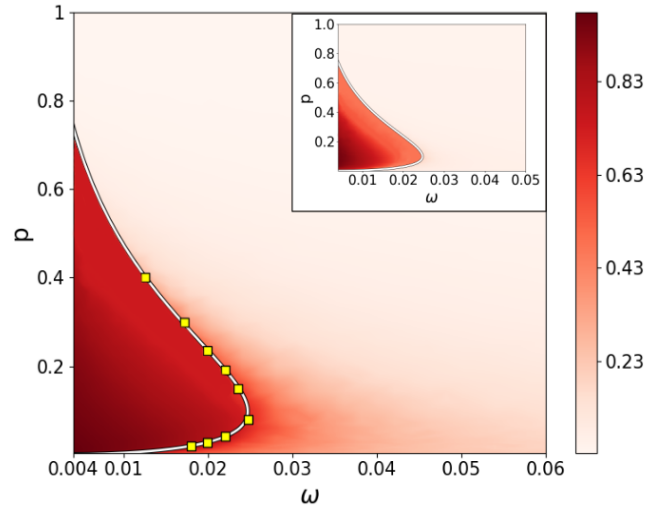


FIG. 1. Density plot of fraction of RTPs in largest cluster. The critical points (symbols) from Table I are plotted along with the best fit critical line  $p_c(\omega)$ . The figure in the inset shows the density plot of the usual order parameter, defined in Eq. (8) of MIPS along with  $p_c(\omega)$ .

elsewhere. Thus a phase separation is expected along with the percolation transition. However, the critical exponents of percolation could be different from that of the MIPS transition. In fact, in context of equilibrium phase transitions, the site-percolation transition of Ising model occurs exactly at the same critical temperature where magnetic transition occurs, but their critical exponents differ [48, 49]. In 2D,

$$\nu_I = 1 = \nu_P, \quad \beta_I = \frac{1}{8} = \frac{12}{5}\beta_P, \quad \gamma_I = \frac{7}{4} = \frac{12}{13}\gamma_P, \quad (1)$$

where  $\nu, \beta, \gamma$  are exponents related to correlation length, order parameter and susceptibility respectively and subscripts  $I, P$  stand for Ising, Percolation. Indeed percolation in Ising model form a different universality class

called interacting percolation or  $Z_2$ -percolation ( $Z_2P$ ) [48, 49] which is different from the well known Ising universality class (IUC) in 2D.

In the RTP model we study in this article, the largest-cluster exhibits a re-entrant percolation transition for small  $\omega$  as we vary  $p$ , the rate of positional diffusion. A macro-cluster appears when  $p$  is increased beyond a threshold, which disappears upon further increase of  $p$ . The density plot of the fraction of particles in largest cluster is shown in Fig. 1. A representative critical line  $p_c(\omega)$  passing through the critical points obtained from numerical simulations separates the two phases. The density plot of usual order-parameter of MIPS transition is shown in the inset of Fig. 1 along with the line  $p_c(\omega)$  which appears to differentiate naturally the PSS from the mixed one. We find that the critical exponents of the percolation transition vary continuously along the critical line (see Table I) while a scaling function remain invariant (see Fig. 3) and matched with the universal scaling function of  $Z_2P$ . Such a scenario is formally termed as super-universality [50, 51]. Thus, the site-percolation critical behaviour of RTPs form a super-universality class of  $Z_2$ -percolation. We also find that the critical exponents of the underlying MIPS-phase transition are related to respective exponents of percolation through Eq. 1 and form a superuniversality class of Ising model.

*The model:* We consider  $N$  run and tumble particles on a square lattice with periodic boundary conditions in both directions, where sites labeled by  $\mathbf{i} \equiv (x, y)$  with  $x, y = 1, 2, \dots, L$  carry an occupation index  $n_{\mathbf{i}} = 0, 1$  representing vacant and occupied sites respectively. Each site can be occupied by at most one particle respecting hard-core or excluded volume repulsion, and thus  $\sum_{\mathbf{i}} n_{\mathbf{i}} = N$ . The particles are labeled by  $m = 1, 2, \dots, N$  and each one carry an internal orientation  $\theta_m = 0, \frac{\pi}{2}, \pi, 3\frac{\pi}{2}$ , which represents a unit vector pointing to one of the four neighbouring sites. The RTPs are allowed to move (run) to the neighbour along their internal orientation with unit rate, and to other three directions with rates  $p$ . Runs along directions other than the particle's own internal orientation adds positional diffusion to the problem, which is essential for having a stable MIPS phase [40, 47]. They can also tumble with rate  $\omega$  by rotating  $\theta_m$  by  $\pm\frac{\pi}{2}$ , and choose a new orientation.

The dynamics of this RTP model is controlled by two parameters: the rate of positional diffusion ( $0 < p < 1$ ) and tumble rate ( $\omega > 0$ ). Earlier numerical simulations [39, 40, 47] have suggested that MIPS transition is not possible in absence of positional diffusion, i.e., when  $p = 0$ , because RTPs cannot escape from micro-clusters. Again, for  $p = 1$ , the model reduces to a system of non-interacting hardcore particles which move in all four directions with the same rate and thus the system remains homogeneously mixed for any  $\omega$ . Absence of an ordered state at  $p = 0$  and  $p = 1$  necessarily indicate that a phase separation transition expected for small  $\omega$  must be

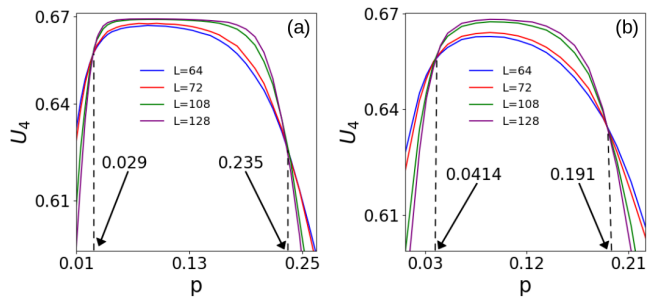


FIG. 2. Binder Cumulant  $U_4$  as a function of  $p$  for (a)  $\omega = 0.020$  and (b)  $\omega = 0.022$ . The two critical points for each  $\omega$ , marked with arrows indicate a re-entrant percolation transition.

re-entrant in the sense that a PSS must appear as  $p$  is increased and it disappears with further increase of  $p$ , which is evident from Fig. 1.

Now we describe, how the critical points and the critical exponents are calculated from numerical simulations. Any configuration of  $N$  RTPs can be viewed as collection of  $K$ -clusters, indexed as  $k = 1, 2, \dots, K$  each containing  $s_k$  number of particles, so that  $\sum_{k=1}^K s_k = N$ . The clusters are formed similar to those in site-percolation problem [52, 53] where two occupied nearest neighbours belong to the same cluster irrespective of their internal orientations. In a mixed state, RTPs are expected to form small clusters whereas in the PSS, there must be at least one macro-size cluster containing a finite-fraction of the total  $N$  particles. Let  $s_{max}$  be the number of particles in the largest cluster. Depending on the density  $\rho = \frac{N}{L^2}$ , it may or may not span the lattice but its presence in the PSS helps us defining the percolation order parameter  $\phi$  and susceptibility  $\chi$ ,

$$\phi = \frac{1}{N} \langle s_{max} \rangle; \chi = \frac{1}{N^2} (\langle s_{max}^2 \rangle - \langle s_{max} \rangle^2), \quad (2)$$

where  $\langle \cdot \rangle$  denotes the steady state average. Note that the same definitions of  $\phi$  and  $\chi$  are used in ordinary percolation [52] and site-percolation in Ising and Potts models [48].

From the Monte Carlo simulations of the system at density  $\rho = \frac{1}{2}$ , we measure  $\phi$ ,  $\chi$  and the Binder-cumulant

$$U_4 = 1 - \frac{\langle s_{max}^4 \rangle}{3 \langle s_{max}^2 \rangle^2} \quad (3)$$

for different  $p$  and  $\omega$ . These calculations are repeated for different system sizes and the critical exponents are determined from the finite size scaling analysis [54–56] described below.

Binder cumulant is independent of the system size [57, 58] and thus, the intersection point of  $U_4$  versus  $p$  (or  $\omega$ ) curves for different  $L$  provide an estimates of  $p_c$  (or  $\omega_c$ ). Figure 2 describes this for  $\omega = 0.020, \omega = 0.022$ . In both cases,  $U_4$  versus  $p$  curves show two intersection points

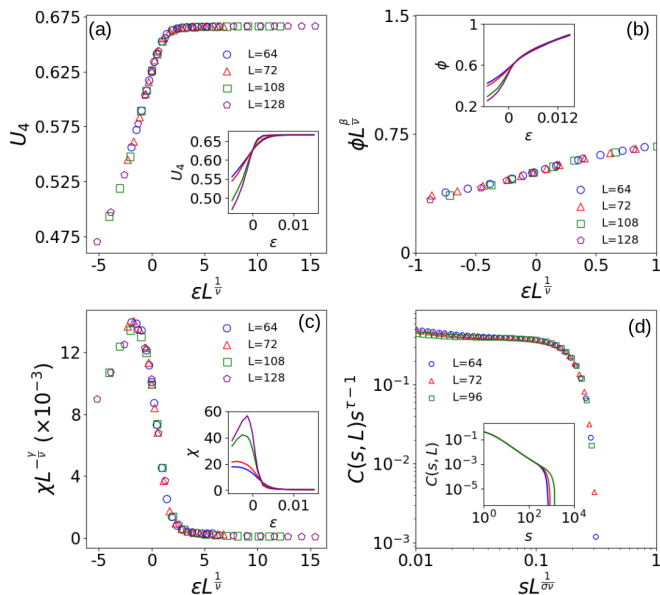


FIG. 3. Finite size scaling at the critical point I  $(p_c, \omega_c) = (0.235, 0.020)$ . (a)  $U_4$ , (b)  $\phi L^{\frac{\beta}{\nu}}$  and (c)  $\chi L^{-\frac{\gamma}{\nu}}$  vs.  $\varepsilon L^{\frac{1}{\nu}}$  where  $\varepsilon = \omega_c - \omega$ . The best collapse are obtained for  $\frac{1}{\nu} = 1.43$ ,  $\frac{\beta}{\nu} = 0.142$ ,  $\frac{\gamma}{\nu} = 1.725$ . (d) Scaling collapse of  $C(s, L)s^{\tau-1}$  vs.  $sL^{\frac{1}{\sigma\nu}}$  yields the exponents  $\tau = 2.075$  and  $\frac{1}{\sigma\nu} = 1.86$ . Insets show the raw data.

indicating a re-entrant transition. In Fig. 2(a) transition from a mixed phase to PSS occurs at  $p_c = 0.029$  and PPS to a mixed phase occurs again at  $p_c = 0.235$ . For  $\omega = 0.022$ , the transitions occur at  $p_c = 0.0414$  and  $0.191$  respectively. Other estimated values of  $(\omega_c, p_c)$  are listed in Table I.

Sl. No.	$p_c$	$\omega_c$	$1/\nu$	$\beta/\nu$	$\gamma/\nu$
I	0.235	0.020(0)	1.43	0.14(2)	1.72(5)
II	0.150	0.023(5)	1.26	0.10(1)	1.75(3)
III	0.080	0.024(7)	1.22	0.09(2)	1.82(4)
IV	0.0290	0.020(0)	1.13	0.06(6)	1.86(8)
V	0.0275	0.019(8)	1.11	0.06(5)	1.87(2)
VI	0.020	0.018(0)	1.10	0.05(5)	1.89(5)
$Z_2P$ [49]	-	-	1	$\frac{5}{96} \approx 0.052$	$\frac{91}{48} \approx 1.896$

TABLE I. Critical points and exponents of percolation transition of RTPs in 2D

Now we vary one of the parameters  $(p, \omega)$  about the critical value  $(p_c, \omega_c)$  and calculate  $\phi, \chi, U_4$  for different  $L$  using Monte Carlo simulations. Using their finite size scaling properties [54–56],

$$\phi = L^{-\frac{\beta}{\nu}} f_\phi(\varepsilon L^{\frac{1}{\nu}}); \chi = L^{\frac{\gamma}{\nu}} f_\chi(\varepsilon L^{\frac{1}{\nu}}); U_4 = f_b(\varepsilon L^{\frac{1}{\nu}}), \quad (4)$$

where  $\varepsilon$  is a measure of distance from the critical point and  $f_{\phi, \chi, b}(\cdot)$  are universal scaling functions, we obtain the exponent ratios  $\frac{1}{\nu}$ ,  $\frac{\gamma}{\nu}$  and  $\frac{\beta}{\nu}$  as the fitting parameters that result in the best scaling collapse. The estimated critical

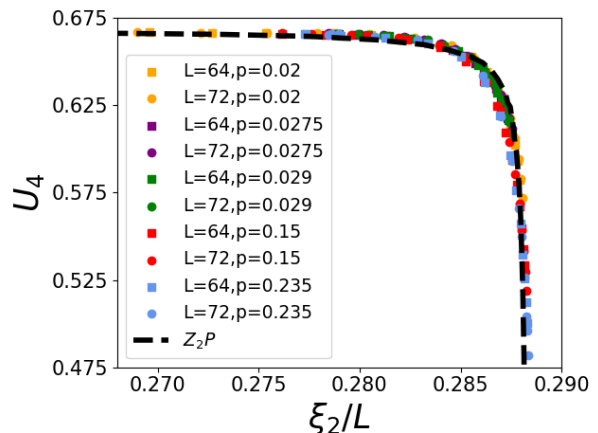


FIG. 4. Plot of  $U_4$  vs.  $\xi_2/L$  parameterized by  $\omega$  for different  $p$  and  $L$ . The dashed line corresponds to the same scaling function of  $Z_2P$  obtained from simulation of Ising percolation.

exponents are listed in Table I. For demonstration, we choose  $p = 0.235$  and vary  $\omega = \omega_c + \varepsilon$  to calculate  $\phi, \chi, U_4$  for different  $L$ . A plot of  $U_4, \phi L^{\frac{\beta}{\nu}}$  and  $\chi L^{-\frac{\gamma}{\nu}}$  as a function of the dimensionless parameter  $\varepsilon L^{\frac{1}{\nu}}$  are shown in Fig. 3(a),(b),(c) respectively. The value of  $\frac{1}{\nu} = 1.43$  that resulted in best collapse of  $U_4$  in Fig. 3(a) is used in Figs. 3(b) and (c) to obtain the best collapse for  $f_\phi(\cdot), f_\chi(\cdot)$  by tuning  $\frac{\beta}{\nu}$  and  $\frac{\gamma}{\nu}$  respectively. The estimated values are  $\frac{\beta}{\nu} = 0.14(2)$  and  $\frac{\gamma}{\nu} = 1.72(5)$ .

To study the cluster properties of RTPs we notice that in the near-critical regime, the distribution of finite clusters  $P(s)$  follow a scaling relation  $P(s, \varepsilon) = s^{-\tau} f(\varepsilon s^\sigma)$  where exponents  $\tau$  and  $\sigma$  obey scaling relations [52],

$$\tau = 2 + \frac{\beta}{\beta + \gamma}, \sigma^{-1} = \beta + \gamma. \quad (5)$$

In finite systems, the correlation length is limited by  $L$ , resulting in  $\varepsilon \sim L^{-\frac{1}{\nu}}$ . Thus, the probability of finding clusters of size  $s$  or more is

$$C(s, L) \equiv \sum_{s'=s}^{\infty} P(s', L) = s^{1-\tau} g(sL^{\frac{1}{\sigma\nu}}). \quad (6)$$

From the Monte Carlo simulations we obtain  $C(s, L)$  at the critical point I  $(p_c, \omega_c) = (0.235, 0.020)$  for different  $L$  and plot  $C(s, L)s^{\tau-1}$  as a function of  $sL^{\frac{1}{\sigma\nu}}$  in Fig. 3(d). We use  $\tau = 2.075$  and  $\frac{1}{\sigma\nu} = 1.86$ , calculated from Eq. (5) and Table I. A good collapse observed here assures that the critical exponents obey the known scaling relations of percolation phenomena [52]. The critical exponents for the other critical points II to VI in Table I are calculated in a similar way, and described in Ref. [59].

*Continuous variation:* The critical exponents listed in Table I vary continuously along the critical line. In each case, however, the scaling relation  $2\beta + \gamma = d\nu$  with  $d = 2$  is satisfied. We have also checked (data not given) that,

within the error limits, independent estimate of exponents  $\tau, \sigma$  satisfy the scaling relations (5). It turns out that the numerical value of the exponents for small  $(p, \omega)$  (say, critical point VI) is very close to the exact values known for  $Z_2$ -percolation transition ( $Z_2P$  in Table I) observed in Ising model [48, 49]. It raises a question if the continuous variation observed here is anyway related to the universality class of  $Z_2P$ .

In fact, recently it was observed [50, 51] that critical phenomena with continuously varying exponents form a super-universality class in the sense that certain scaling function remain invariant along the critical line and they match with that of the ordinary universality class. One such RG-invariant scaling function is  $U_4 = F\left(\frac{\xi_2}{L}\right)$  which relates the Binder cumulant with second-moment correlation length  $\xi_2$ ,

$$(\xi_2)^2 = \frac{\int_0^\infty r^2 g(r) dr}{\int_0^\infty g(r) dr}; \quad g(r) = \langle n_i n_{i+r} \rangle - \langle n_i \rangle \langle n_{i+r} \rangle. \quad (7)$$

For RTPs we obtain  $\xi_2$  and  $U_4$  as functions of  $\omega$  using Monte Carlo simulations, for different  $p, L$ . The plots of  $U_4$  vs.  $\frac{\xi_2}{L}$  for many different  $(p, \omega, L)$  values plotted in Fig. 4 fall on a universal function  $F(\cdot)$  which is no different from the same obtained for  $Z_2P$  universality class (dashed line). We conclude that the percolation transition of RTPs belong to the super-universality class of  $Z_2$ -percolation. Then it is suggestive, following Eq. (1), that the MIPS transition may have critical exponents  $\beta' = \frac{12}{5}\beta, \nu' = \nu, \gamma' = \frac{12}{13}\gamma$ . To verify, we consider a rect-

angular system with  $L_x = L, L_y = \frac{L}{2}$  and study phase separation transition about the critical points I and III in Table I using an order parameter similar to one discussed in Refs. [47, 60, 61],

$$\phi' = \frac{2}{L_x L_y} \sum_{x=1}^{L_x} |N_x - \rho L_y|; \quad N_x = \sum_{y=1}^{L_y} n_{x,y}, \quad (8)$$

where  $N_x$  is the total number of particles at lattice sites  $\mathbf{i} \equiv (x, y)$  with the same  $x$ -coordinate. From Monte Carlo simulation of the model we calculate  $\bar{\phi} = \langle \phi' \rangle$  and  $\bar{\chi} = \langle \phi'^2 \rangle - \langle \phi' \rangle^2$  as a function of  $\omega$ , keeping  $p$  fixed. The plots in Fig. 5 shows that the data for different  $L$  values collapse following the finite size scaling,

$$\phi' = L^{-\frac{\beta'}{\nu}} f'_\phi(\varepsilon L^{\frac{1}{\nu}}); \quad \chi' = L^{\frac{\gamma'}{\nu}} f'_\chi(\varepsilon L^{\frac{1}{\nu}}), \quad (9)$$

when we use  $\beta' = \frac{12}{5}\beta, \gamma' = \frac{12}{13}\gamma$  with  $\frac{1}{\nu}, \frac{\beta'}{\nu}, \frac{\gamma'}{\nu}$  taken from Table I. Note that critical points of the MIPS transition are taken to be same as the corresponding percolation transition because it is evident from the density plot of  $\phi'$  in the inset of Fig. 8 that the percolation critical line naturally separates the mixed state from the PSS. Thus, the MIPS transition of RTPs in  $\omega$ - $p$  plane lead to continuous variation of the critical exponents  $\beta', \gamma', \nu'$  obeying the scaling relation  $d\nu' = 2\beta' + \gamma'$ . Thus, we believe that the MIPS transition of RTPs in 2D belong to Ising super-universality class. Note that as  $(\omega, p) \rightarrow (0, 0)$  the critical exponents of MIPS transition approach the Ising exponents following Eq. (1). This result is consistent with the Ising critical behavior reported in RTP models studied earlier for small  $p, \omega$  [44–46].

In conclusion, we study percolation transition of run and tumble particles on a square lattice, where clusters are formed by joining occupied nearest neighbours irrespective of their internal orientation. We find that the system with a small tumbling rate  $\omega$  undergoes a re-entrant percolation transition when rate of positional diffusion  $p$  is increased. The transition belongs to the super-universality class of  $Z_2$  percolation: all critical exponents of the transition vary continuously along the critical line in  $\omega$ - $p$  plane but a scaling function  $U_4 = F\left(\frac{\xi_2}{L}\right)$  remains invariant. Thus the percolation transition belongs to the superuniversality class of  $Z_2P$ . Since any phase separated state must contain at least one macro cluster, motility induced phase separation transition of RTPs must occur at the critical point of percolation-transition, and it does. The critical exponents, however, differ and they are related to percolation exponents by a constant multiplicative factor, known from the relation of Ising model and  $Z_2$  percolation.

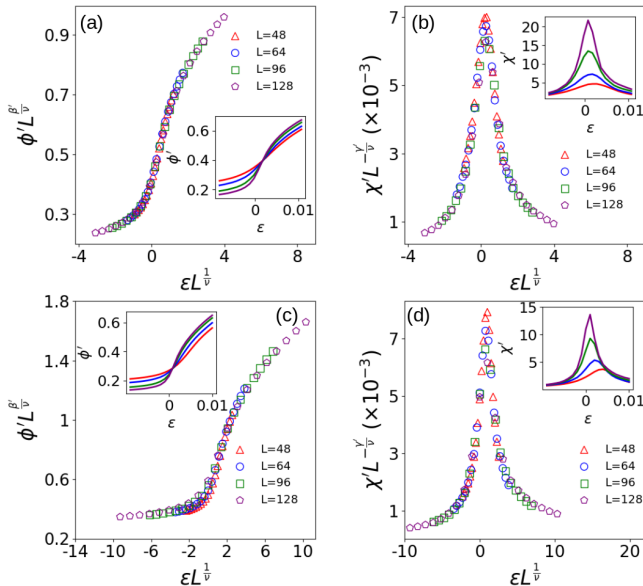


FIG. 5. Finite size scaling collapse of MIPS order parameter  $\phi'$  and susceptibility  $\chi'$ . (a), (b) correspond to the critical point IV resulting in  $\frac{\beta'}{\nu} = 0.216, \frac{\gamma'}{\nu} = 1.68$ . The same for the critical point VI are shown in (c), (d) with resulting exponents  $\frac{\beta'}{\nu} = 0.336, \frac{\gamma'}{\nu} = 1.59$ .

\* pkmohanty@iiserkol.ac.in

- [1] S. Ramaswamy, *Annu. Rev. Cond. Mat. Phys.*, **1**, 323 (2010), doi:10.1146/annurev-conmatphys-070909-104101.
- [2] M. E. Cates, *Rep. Prog. Phys.* **75**, 042601 (2012), doi:10.1088/0034-4885/75/4/042601.
- [3] M. C. Marchetti, J.F. Joanny, S. Ramaswamy, T. B. Liverpool, J. Prost, M. Rao, R. A. Simha, *Rev. Mod. Phys.* **85** 1143 (2013), doi:10.1103/RevModPhys.85.1143.
- [4] G. de Magistris, D. Marenduzzo, *Physica A* **418**, 65 (2015), doi:10.1016/j.physa.2014.06.061.
- [5] C. Bechinger, R. D. Leonardo, H. Löwen, C. Reichhardt, G. Volpe, G. Volpe, *Rev. Mod. Phys.* **88**, 045006 (2016) doi:10.1103/RevModPhys.88.045006.
- [6] R. Alert and X. Trepat, *Annu. Rev. Condens. Matter Phys.* **11**, 77 (2020), doi:10.1146/annurev-conmatphys-031218-013516.
- [7] M. Ballerini, N. Cabibbo, R. Candelieri, A. Cavagna, E. Cilibani, I. Giardinà, V. Lecomte, A. Orlandi, G. Parisi, A. Procaccini et al., *Proc. Natl. Acad. Sci. U.S.A.* **105**, 1232 (2008), doi:10.1073/pnas.0711437105.
- [8] A. J. Ward, D. J. Sumpter, I. D. Couzin, P. J. Hart, and J. Krause, *Proc. Natl. Acad. Sci.* **105**, 6948 (2008), doi:10.1073/pnas.0710344105.
- [9] A. Cavagna, D. Conti, C. Creato, L. Del Castello, I. Giardinà, T. S. Grigera, S. Melillo, L. Parisi, and M. Viale, *Nat. Phys.* **13**, 914 (2017), doi:10.1038/nphys4153.
- [10] A. Be'er, B. Ilkanaiv, R. Gross, D. B. Kearns, S. Heidenreich, M. Bär, and G. Ariel, *Commun. Phys.* **3**, 66 (2020), doi:10.1038/s42005-020-0327-1.
- [11] F. Peruani, J. Starruss, V. Jakovljevic, L. Sogaard-Andersen, A. Deutsch, M. Bär, *Phys. Rev. Lett.* **108**, 098102 (2012), doi:10.1103/PhysRevLett.108.098102.
- [12] H. C. Berg, *E. coli in Motion*, Springer, NY (2004), doi:10.1007/b97370.
- [13] M. Polin, I. Tuval, K. Drescher, J. P. Gollub, and R. E. Goldstein, *Science*, **325**, 487, (2009), doi:10.1126/science.1172667.
- [14] J. Tailleur, M.E. Cates, *Phys. Rev. Lett.* **100**, 218103 (2008), doi:10.1103/PhysRevLett.100.218103.
- [15] M. E. Cates and J. Tailleur, *Europhys. Lett.* **101** 20010 (2013), doi:10.1209/0295-5075/101/20010
- [16] M. E. Cates and J. Tailleur, *Annu. Rev. Cond. Mat. Phys.*, **6**, 219 (2015), doi:10.1146/annurev-conmatphys-031214-014710.
- [17] Y. Fily, M.C. Marchetti, *Phys. Rev. Lett.* **108**, 235702 (2012), doi:10.1103/PhysRevLett.108.235702.
- [18] Y. Fily, S. Henkes, M.C. Marchetti, *Soft Matter* **10**, 2132 (2014) doi:10.1039/C3SM52469H.
- [19] G. S. Redner, M. F. Hagan and A. Baskaran, *Phys. Rev. Lett.* **110**, 055701 (2013), doi:10.1103/PhysRevLett.110.055701.
- [20] J. Stenhammar, A. Tiribocchi, R.J. Allen, D. Marenduzzo, M.E. Cates, *Phys. Rev. Lett.* **111**, 145702 (2013), doi:10.1103/PhysRevLett.111.145702.
- [21] G. Gonnella, A. Lamura, A. Suma, *Int. J. Mod. Phys. C* **25**, 1441004 (2014), doi:10.1142/S0129183114410046.
- [22] A. Suma, D. Marenduzzo, G. Gonnella, E. Orlandini, *Europhys. Lett.* **108**, 56004 (2014), doi:10.1209/0295-5075/108/56004.
- [23] D. Levis, L. Berthier, *Phys. Rev. E* **89**, 062301 (2014), doi:10.1103/PhysRevE.89.062301.
- [24] R. Wittkowski, A. Tiribocchi, J. Stenhammar, R. Allen, D. Marenduzzo, M. Cates, *Nat. Commun.* **5**, 4351 (2014), doi:10.1038/ncomms5351.
- [25] M. Kourbane-Houssene, C. Erignoux, T. Bodineau, and J. Tailleur, *Phys. Rev. Lett.* **120**, 268003 (2018), doi:10.1103/PhysRevLett.120.268003.
- [26] Y. Fily and M. C. Marchetti, *Phys. Rev. Lett.* **108**, 235702 (2012), doi:10.1103/PhysRevLett.108.235702.
- [27] J. Bialkèl, H. Löwen and T. Speck, *Europhys. Lett.* **103**, 30008 (2013), doi:10.1209/0295-5075/103/30008.
- [28] F. Schweitzer *Eur. J. Phys.* **40**, 014003 (2019).
- [29] A. Ziepke, I. Maryshev, I. S. Aranson, and E. Frey, *Nat. Commun.* **13**, 6727 (2022), doi:10.1038/s41467-022-34484-2
- [30] A. G. Thompson, J. Tailleur, M. E. Cates, and R. A. Blythe, *J. Stat. Mech.*, P02029 (2011), doi:10.1088/1742-5468/2011/02/P02029.
- [31] A. B. Slowman, M. R. Evans, and R. A. Blythe, *Phys. Rev. Lett.* **116**, 218101 (2016), doi:10.1103/PhysRevLett.116.218101.
- [32] E. Mallmin, R. A. Blythe, and M. R. Evans, *J. Stat. Mech.*, 013204 (2019), doi:10.1088/1742-5468/aaf631.
- [33] R. Dandekar, S. Chakraborti, and R. Rajesh, *Phys. Rev. E* **102**, 062111 (2020), doi:10.1103/PhysRevE.102.062111.
- [34] I. Mukherjee, A. Raghu, P. K. Mohanty, *SciPost Phys.* **14**, 165 (2023), doi:10.21468/SciPostPhys.14.6.165.
- [35] J. Palacci, B. Abecassis, C. Cottin-Bizonne, C. Ybert, and L. Bocque, *Phys. Rev. Lett.* **104**, 138302 (2010), doi:10.1103/PhysRevLett.104.138302.
- [36] J. Palacci, S. Sacanna, S.-H. Kim, G.-R. Yi, D. J. Pine and P. M. Chaikin, *Phil. Trans. R. Soc. A* **372**, 20130372 (2014), doi:10.1098/rsta.2013.0372.
- [37] P. Kushwaha, V. Semwal, S. Maity, S. Mishra, and V. Chikkadi *Phys. Rev. E* **108**, 034603 (2023) doi:10.1103/PhysRevE.108.034603.
- [38] P. Kushwaha, S. Maitya, A. Menon, R. Chelakkot and V. Chikkadi, *Soft Matter* (2024), doi:10.1039/D4SM00305E.
- [39] R. Soto and R. Golestanian, *Phys. Rev. E* **89**, 012706 (2014), doi:10.1103/PhysRevE.89.012706.
- [40] S. Whitelam, K. Klymko, D. Mandal, *J. Chem. Phys.* **148**, 154902 (2018), doi:10.1063/1.5023403.
- [41] A. P. Solon and J. Tailleur *Phys. Rev. E* **92**, 042119 (2015).
- [42] N. Sepúlveda and R. Soto, *Phys. Rev. E* **94**, 022603 (2016), doi:10.1103/PhysRevE.94.022603.
- [43] J. T. Siebert, F. Dittrich, F. Schmid, K. Binder, T. Speck, and P. Virnau, *Phys. Rev. E* **98**, 030601(R) (2018), doi:10.1103/PhysRevE.98.030601.
- [44] B. Partridge and C. F. Lee, *Phys. Rev. Lett.* **123**, 068002 (2019), doi:10.1103/PhysRevLett.123.068002.
- [45] C. Maggi, M. Paoluzzi, A. Crisanti, E. Zaccarelli, and N. Gnan, *Soft Matter* **17**, 38072021 (2021), doi:10.1039/D0SM02162H.
- [46] F. Dittrich, T. Speck and P. Virnau, *Eur. Phys. J. E* **44**, 53 (2021), doi:10.1140/epje/s10189-021-00058-1.
- [47] C. G. Ray, I. Mukherjee, P. K. Mohanty, *arXiv:2307.03216* doi:10.48550/arXiv.2307.03216
- [48] S. Fortunato, *Phys. Rev. B* **66**, 054107(2002).
- [49] A. L. Stella and C. Vanderzande, *Phys. Rev. Lett.* **62**, 1067 (1989) doi:10.1103/PhysRevLett.62.1067
- [50] C. Bonati, A. Pelissetto, and E. Vicari, *Phys. Rev. Lett.* **123**, 232002 (2019), doi:10.1103/PhysRevLett.123.232002.
- [51] I. Mukherjee, P. K. Mohanty *Phys. Rev. B* **108**, 174417 (2023)doi:10.1103/PhysRevB.108.174417
- [52] D. Stauffer, *Phys. Rep.* **54**, 1 (1979).

- [53] D. Stauffer and A. Aharony, *Introduction To Percolation Theory*, 2<sup>nd</sup> ed., Taylor & Francis Ltd., India (1994).
- [54] K. Binder, D. W. Heermann, *Monte Carlo Simulation in Statistical Physics* (5th Ed.) Springer Berlin, 2010.
- [55] K. Binder, Phys. Rev. Lett. **47**, 693 (1981), doi: 10.1103/PhysRevLett.47.693.
- [56] V. Privman (ed.), *Finite-Size Scaling and Numerical Simulations of Statistical Systems*, World Scientific, Singapore, 1990.
- [57] D. P. Landau and K. Binder, *A Guide to Monte Carlo Simulations in Statistical Physics* (Cambridge University Press, Cambridge, UK, 2014).
- [58] E. Luijten, M. E. Fisher, and A. Z. Panagiotopoulos, Phys. Rev. Lett. **88**, 185701 (2002), doi: 10.1103/PhysRevLett.88.185701.
- [59] See the Supplemental Materials for details of the simulation and additional results in support of our claims.
- [60] J. Marro, J. L. Vallés, and J. M. González-Miranda, Phys. Rev. B **35**, 3372 (1987), doi: 10.1103/PhysRevB.35.3372.
- [61] E. V. Albano and G. Saracco, Phys. Rev. Lett. **88**, 145701 (2002), doi:10.1103/PhysRevLett.88.145701
- [62] J. Ashkin and E. Teller, *Phys. Rev.* **64**, 178 (1943).

# Supplemental Material: Site-percolation transition of run-and-tumble particles

Soumya K. Saha, Aikya Banerjee, and P. K. Mohanty\*

*Department of Physical Sciences, Indian Institute of Science Education and Research Kolkata, Mohanpur, 741246 India.*

The Supplemental Material provides additional results to support and strengthen the claims of the article. First we introduce the model for completeness and then describe the simulation methods in detail. We also provide the finite size scaling collapse for all the critical points, mentioned in the main text.

## I. MODEL : DESCRIPTION AND DYNAMICS

We consider  $N$  run and tumble particles (RTPs) on a two dimensional square lattice of size  $L \times L$ . Each site  $\mathbf{i} \equiv (x, y)$  with  $x, y = 1, 2, \dots, L$  carries a site variable  $n_{\mathbf{i}} = 0, 1$  representing absence, presence of a particle so that  $\sum_{\mathbf{i}} n_{\mathbf{i}} = N$ . Clearly particles experience hard-core repulsion and occupation of two particles at any site is strictly prohibited. Figure 1(a) shows a representative configuration of  $N = 15$  RTPs on a  $9 \times 9$  square lattice. The RTPs are associated with an internal orientation that points to one of the nearest neighbours, denoted by a long arrow. Particles move along their intrinsic direction with unit rate, and along the other three directions (represented by short arrows) with rates  $p < 1$ . This run-dynamics is shown in Fig. 1(b). In addition, as shown in Fig. 1(c), the RTPs can tumble and change their intrinsic orientation by rotating clockwise or anti-clockwise by an angle  $\pi/2$ , each with rate  $\omega$ .

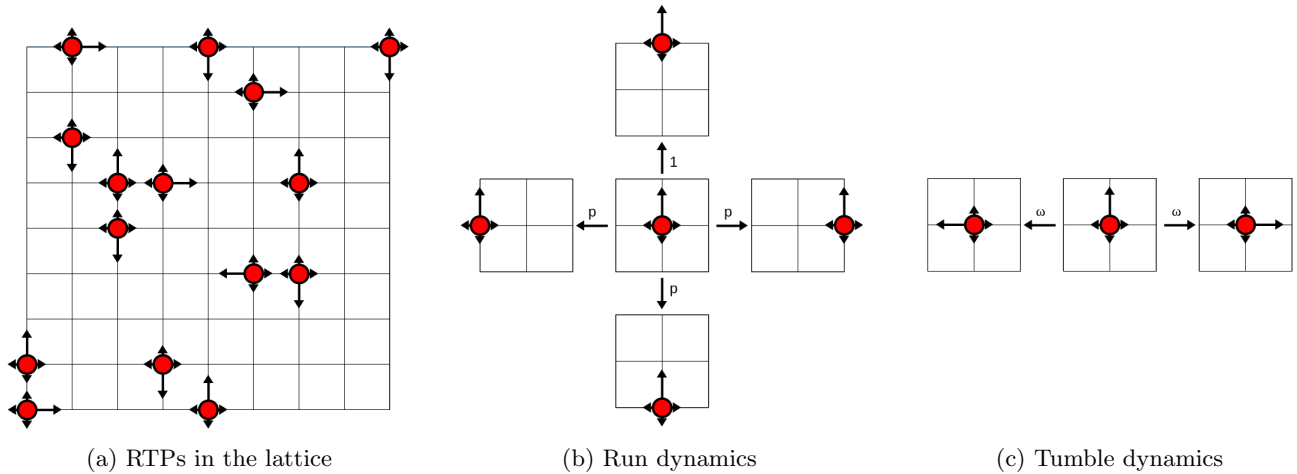


FIG. 1: Illustration of the model

## II. DETAILS OF THE SIMULATION

To do Monte-Carlo simulations, we start by placing  $N$  particles on the sites  $(x, y) \equiv \mathbf{i}$  of a square lattice randomly and independently, such that each site is occupied by at most one particle. To each particle we assign an orientation - a unit vector  $\delta$  pointing to one of the nearest neighbours. A particle is chosen at random from the lattice. Say, it's location is  $\mathbf{i}$  and internal orientation  $\delta_{\mathbf{i}}$ .

\*Electronic address: pkmohanty@iiserkol.ac.in

In the Monte-Carlo dynamics the with following events are attempted with different probabilities.

$$\text{prob. } \Delta t : (n_i = 1, n_{i+\delta_i} = 0) \rightarrow (n_i = 0, n_{i+\delta_i} = 1) \quad (1)$$

$$\text{prob. } p\Delta t : (n_i = 1, n_{i+\delta_1} = 0) \rightarrow (n_i = 0, n_{i+\delta_1} = 1) \quad (2)$$

$$\text{prob. } p\Delta t : (n_i = 1, n_{i+\delta_2} = 0) \rightarrow (n_i = 0, n_{i+\delta_2} = 1) \quad (3)$$

$$\text{prob. } p\Delta t : (n_i = 1, n_{i+\delta_3} = 0) \rightarrow (n_i = 0, n_{i+\delta_3} = 1) \quad (4)$$

$$\text{prob. } \omega\Delta t : \delta_i \rightarrow \delta_1 \quad (5)$$

$$\text{prob. } \omega\Delta t : \delta_i \rightarrow \delta_3 \quad (6)$$

$$\text{prob. } 1 - (1 + 3p + 2\omega)\Delta t : \text{do nothing,} \quad (7)$$

where  $\delta_k$  with  $k = 1, 2, 3$  are unit vectors obtained from rotating  $\delta_i$  by  $k\frac{\pi}{2}$ . Equation (1) makes particle to run along their internal orientation, whereas Eqs. (2), (3), and (4) generate positional diffusion of RTPs by allowing them to move along directions another than their internal orientation. Equations (5) and (6) represents tumbling. Finally Eq. (7) assures that only of the above six events happen at any point of time; the time is then advanced by  $t \rightarrow t + \frac{\Delta t}{N}$ .

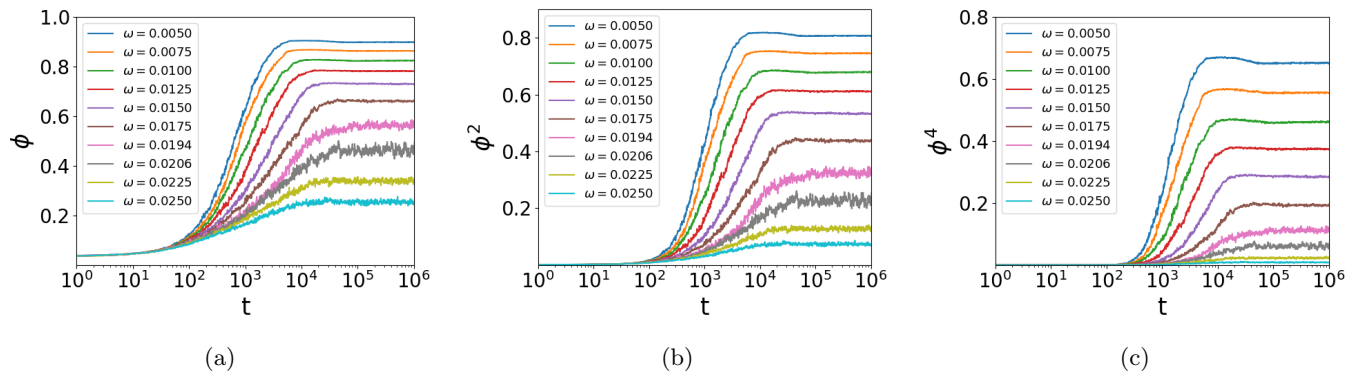


FIG. 2: Time evolution of (a) $\phi$ , (b) $\phi^2$ , and (c) $\phi^4$  for  $p = 0.235$  and various values of  $\omega$

Our aim is to calculate the steady state average of the largest cluster. A cluster is defined in a way similar to the clusters defined in the site percolation problem - two particles separated by one lattice unit belong to same cluster. For example the configuration in Fig. 1(a) has seven isolated particles, one cluster of size  $s = 3$  and three clusters of size  $s = 2$ ; the maximum size is  $s_{max} = 3$ . To calculate the steady state averages  $\langle s_{max} \rangle$ ,  $\langle s_{max}^2 \rangle$ ,  $\langle s_{max}^4 \rangle$  we first estimate the relaxation time  $\tau$ . For the parameters chosen in this work we have found that  $\tau < 10^7$ , which is is described for a system of size  $L = 128$  in Fig. 2 Once in steady state we calculate  $\langle s_{max} \rangle$ ,  $\langle s_{max}^2 \rangle$ ,  $\langle s_{max}^4 \rangle$  by averaging the data over  $10^8$  or more samples. Using these, we calculate the order parameter  $\phi = \langle s_{max} \rangle$ , the susceptibility  $\chi = \langle s_{max}^2 \rangle - \langle s_{max} \rangle^2$  and the binder cumulant  $U_4 = 1 - \frac{\langle s_{max}^4 \rangle}{3\langle s_{max}^2 \rangle^2}$ .

The model has two parameters:  $p, \omega$ , the density is fixed at  $\rho = \frac{N}{L^2} = \frac{1}{2}$ . In  $\omega \rightarrow \infty$  limit, the persistent nature of RTPs is lost and the dynamics reduces to diffusion of hardcore passive particles on a lattice, generating all possible configurations with equal probability. The phase separated state, if any should be visible when  $\omega$  is lowered below a critical threshold  $\omega_c$  which is a function of  $p$ . To calculate the critical point  $(p_c, \omega_c)$  we set  $p$  at some specific value and measure  $U_4$  as a function of  $\omega$ , for three different system sizes  $L = 64, 72, 108, 128$ . Since  $U_4$  is independent of the system size at  $w = w_c$ , the crossing point of these curves give us a good estimate of  $\omega_c$ . Alternatively one can also estimate  $p_c$  from  $U_4$  vs.  $p$  curves for a fixed  $\omega$ , which is done in Fig. 2 of main text for (a)  $\omega = 0.02$  and  $\omega = 0.022$ . All the estimated critical points are listed in Table I. of main text.

### A. The phase diagram

To obtain the phase diagram we plot the heat map of the order parameter  $\langle s_{max} \rangle$  in  $(\omega, p)$ - plane in Fig. 3(a) where the darker region represent a phase separated state that contains a macroscopic-cluster. The line that separates the mixed phase from the phase-separated state is obtained from a best fit of the the critical points obtained from simulations. Clearly, a re-entrant percolation transition is observed when  $p$  is varied keeping  $\omega$  fixed. With increased  $p$  percolated state appears and then then it disappears with further increase of  $p$ . Typical largest clusters of the system are shown in Fig. 3(b) at nine different points  $(p = 0.02, 0.08, 0.235) \times (\omega = 0.012, 0.022, 0.032)$  marked as



circles. The largest cluster is macroscopic (and spans the lattice) for all three values of  $p$  when  $\omega = 0.012$ . Whereas for  $\omega = 0.022$ , the largest cluster is small for  $p = 0.08$ , it becomes much denser at  $p = 0.022$  and becomes sparsely connected again at a larger value of  $p = 0.235$  indicating the re-entrant nature of the transition.

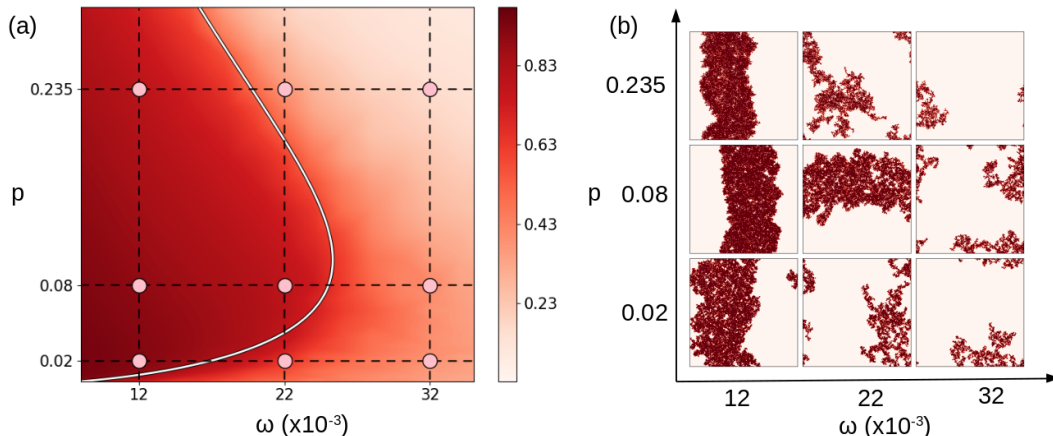


FIG. 3: (a) Phase diagram: The solid line, obtained from the best fit of the critical points, separates the mixed phase from phase separated state. The background is the heat map of the order parameter. (b) Typical largest clusters at nine different points ( $p = 0.02, 0.08, 0.235$ )  $\times$  ( $\omega = 0.012, 0.022, 0.032$ ) marked as circles in (a).

### B. Critical exponents from finite size scaling

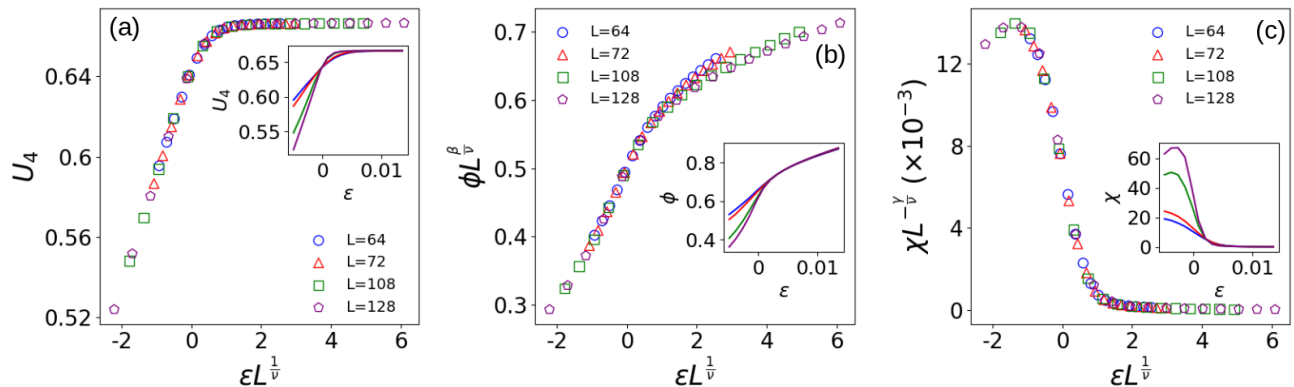


FIG. 4: Critical point II.  $(p_c, \omega_c) = (0.150, 0.0235)$ : (a)  $U_4$ , (b)  $\phi L^{\frac{\beta}{\nu}}$  and (c)  $\chi L^{-\frac{\gamma}{\nu}}$  as a function of  $\varepsilon L^{\frac{1}{\nu}}$ . The best collapse is obtained for  $\frac{1}{\nu} = 1.26$ ,  $\frac{\beta}{\nu} = 0.10$ ,  $\frac{\gamma}{\nu} = 1.75$ . The inset shows raw data,  $U_4, \phi, \chi$  vs.  $\varepsilon$ .

To obtain the static critical exponents  $\nu, \beta, \gamma$  we employ the finite size scaling analysis,

$$\phi = L^{-\frac{\beta}{\nu}} f_{\phi}(\varepsilon L^{\frac{1}{\nu}}); \chi = L^{\frac{\gamma}{\nu}} f_{\chi}(\varepsilon L^{\frac{1}{\nu}}); U_4 = f_b(\varepsilon L^{\frac{1}{\nu}}). \quad (8)$$

For one of the critical point I.  $(p_c, \omega_c) = (0.235, 0.020)$  Figs. 3(a), (b) and (c) in the main text show respectively the scaling collapse of  $\phi L^{\frac{\beta}{\nu}}$ ,  $\chi L^{-\frac{\gamma}{\nu}}$  and  $U_4$  as a function of  $\varepsilon L^{\frac{1}{\nu}}$ . Similar scaling collapse for the other critical points (II to VI mentioned in Table I of the main text) are shown respectively in Figs. 4 to 8.

### C. Critical behaviour in $p$ - direction

In a two parameter space there are two independent direction. At any critical point the critical exponents can be obtained from varying one of the paramters keeping the other fixed. So far we have done the finite size scaling analysis

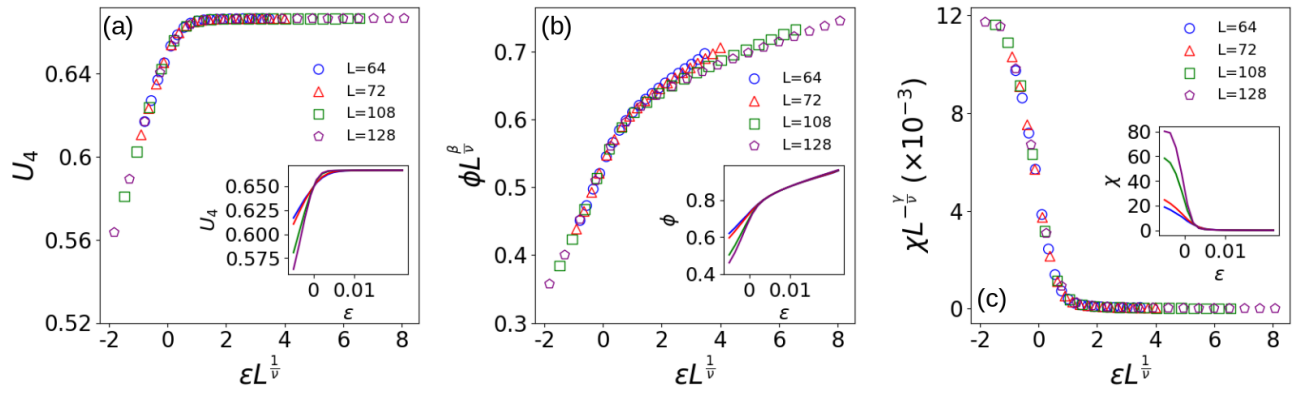


FIG. 5: Critical point III.  $(p_c, \omega_c) = (0.080, 0.0247)$ : (a)  $U_4$ , (b)  $\phi L^{\frac{\beta}{\nu}}$  and (c)  $\chi L^{-\frac{\gamma}{\nu}}$  as a function of  $\varepsilon L^{\frac{1}{\nu}}$ . The best collapse is obtained for  $\frac{1}{\nu} = 1.22$ ,  $\frac{\beta}{\nu} = 0.09$ ,  $\frac{\gamma}{\nu} = 1.82$ . The inset shows raw data,  $U_4, \phi, \chi$  vs.  $\varepsilon$ .

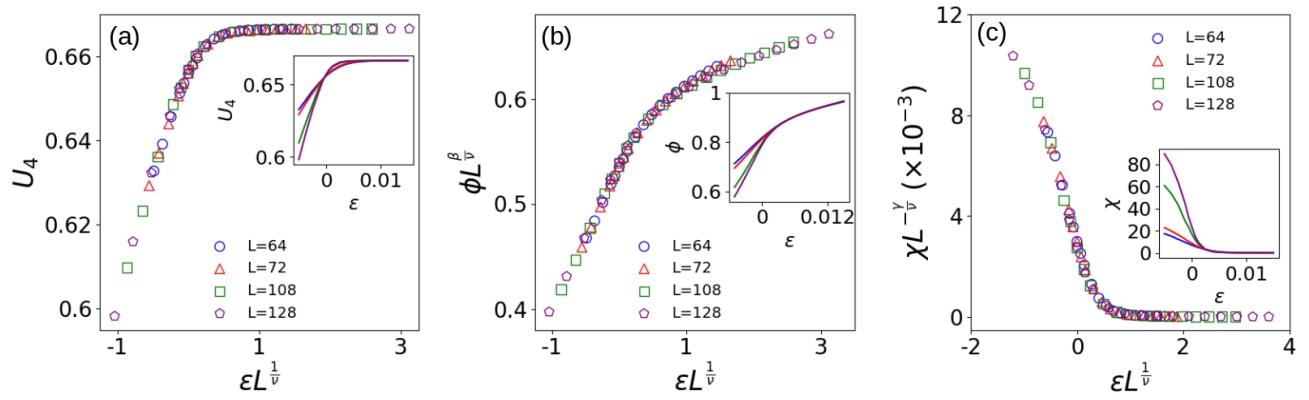


FIG. 6: Critical point IV.  $(p_c, \omega_c) = (0.029, 0.020)$ : (a)  $U_4$ , (b)  $\phi L^{\frac{\beta}{\nu}}$  and (c)  $\chi L^{-\frac{\gamma}{\nu}}$  as a function of  $\varepsilon L^{\frac{1}{\nu}}$ . The best collapse is obtained for  $\frac{1}{\nu} = 1.13$ ,  $\frac{\beta}{\nu} = 0.066$ ,  $\frac{\gamma}{\nu} = 1.868$ . The inset shows raw data,  $U_4, \phi, \chi$  vs.  $\varepsilon$ .

by varying  $\omega$  for a fixed  $p$ . For consistency, we consider one of the critical point  $(p_c, \omega_c) = (0.235, 0.020)$ , fix  $\omega = 0.02$  and study the critical behaviour by varying  $p$ . Now the scaling functions depend on  $\Delta = p_c - p$ ,

$$\phi = L^{-\frac{\beta}{\nu}} \tilde{f}_\phi(\Delta L^{\frac{1}{\nu}}); \quad \chi = L^{\frac{\gamma}{\nu}} \tilde{f}_\chi(\Delta L^{\frac{1}{\nu}}); \quad U_4 = \tilde{f}_b(\Delta L^{\frac{1}{\nu}}). \quad (9)$$

A plot of  $\phi L^{\frac{\beta}{\nu}}$ ,  $\chi L^{-\frac{\gamma}{\nu}}$  and  $U_4$  as a function of  $\Delta L^{\frac{1}{\nu}}$  is shown in Fig. 9 where  $\frac{\beta}{\nu}$ ,  $\frac{\gamma}{\nu}$  and  $\frac{1}{\nu}$  are tuned to a value that gives the best collapse. We find that the critical exponents  $\frac{1}{\nu} = 1.43$ ,  $\frac{\beta}{\nu} = 0.14$ ,  $\frac{\gamma}{\nu} = 1.72$  obtained previously by varying  $\varepsilon$ , gives rise to best data collapse.

### III. MOTILITY INDUCED PHASE SEPARATION TRANSITION

The RTPs undergo a percolation transition when  $\omega$  is lowered below a critical threshold value  $\omega_c$  that depends on  $p$ . This percolation transition belong to the super universality class of  $Z_2$  percolation. Should we expect that the motility induced phase separation transition of RTPs also occur at  $\omega_c$ ? In fact, in 2D Ising Model a percolation transition occurs exactly at the same critical temperature  $T_c$  where the system phase transit from being a para-magnet to a ferromagnet. The critical behaviour of percolation transition form a new universality class called  $Z_2$ -percolation which is different from Ising universality class (IUC). In a similar way, if MIPS occurs in RTP model when  $\omega$  is lowered below  $\omega_c$ , what could be a suitable order parameter to characterize such a transition? We use the order parameter suggested in Ref.[3]. It is well-known that in a rectangular system of length  $L_x$  and height  $L_y$ , the high density phase boundaries align in the shorter direction. Fig. 10(a) shows a typical high density phase (shaded)

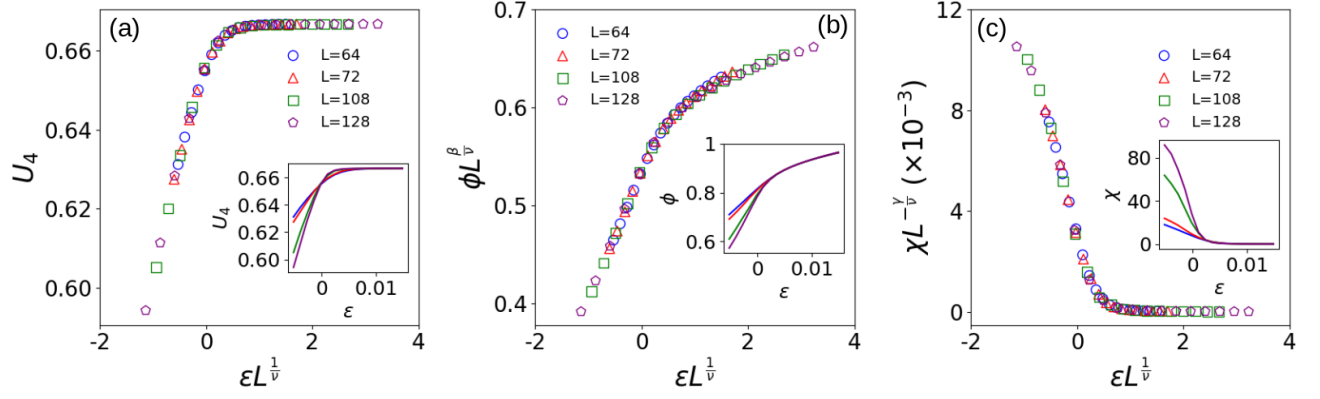


FIG. 7: Critical point V.  $(p_c, \omega_c) = (0.0275, 0.019)$ : (a)  $U_4$ , (b)  $\phi L^{\frac{\beta}{\nu}}$  and (c)  $\chi L^{-\frac{\gamma}{\nu}}$  as a function of  $\varepsilon L^{\frac{1}{\nu}}$ . The best collapse is obtained for  $\frac{1}{\nu} = 1.11$ ,  $\frac{\beta}{\nu} = 0.065$ ,  $\frac{\gamma}{\nu} = 1.87$ . The inset shows raw data,  $U_4, \phi, \chi$  vs.  $\varepsilon$ .

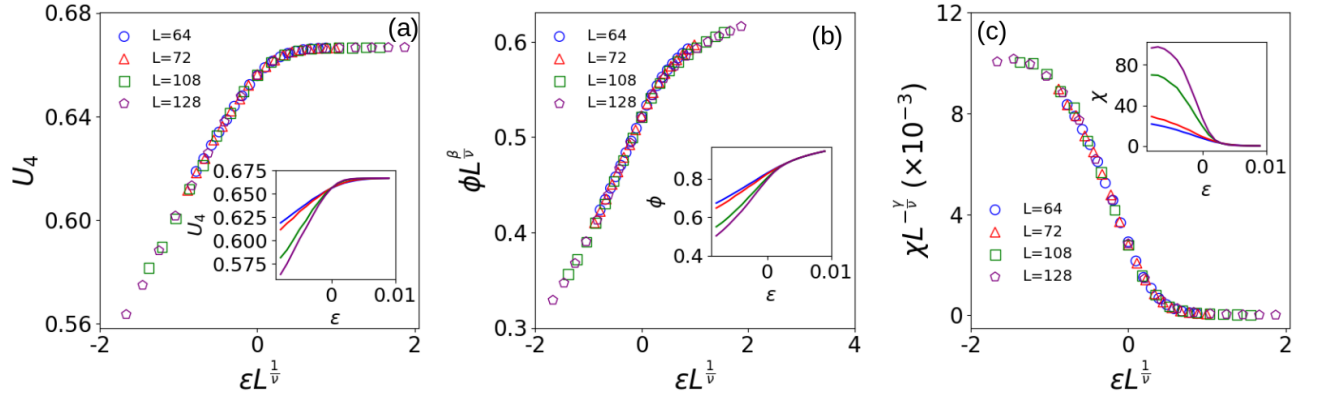


FIG. 8: Critical point VI.  $(p_c, \omega_c) = (0.020, 0.018)$ : (a)  $U_4$ , (b)  $\phi L^{\frac{\beta}{\nu}}$  and (c)  $\chi L^{-\frac{\gamma}{\nu}}$  as a function of  $\varepsilon L^{\frac{1}{\nu}}$ . The best collapse is obtained for  $\frac{1}{\nu} = 1.10$ ,  $\frac{\beta}{\nu} = 0.055$ ,  $\frac{\gamma}{\nu} = 1.89$ . The inset shows raw data,  $U_4, \phi, \chi$  vs.  $\varepsilon$ .

in a system where  $L_x = 2L_y$ . Then the order parameter  $\phi'$  is defined as [3],

$$\phi' = \frac{2}{L_x L_y} \sum_{x=1}^{L_x} |N_x - \rho L_y|; \quad N_x = \sum_{y=1}^{L_y} n_{x,y}, \quad (10)$$

where  $N_x$  is the total number of particles at lattice sites  $\mathbf{i} \equiv (x, y)$  with the same  $x$ -coordinate. A schematic representation of how  $\phi'$  quantifies a typical clustered configuration is shown in Fig 10.

Using finite size scaling of the standard order parameter and the corresponding susceptibility at the critical points IV and VI (refer Table 1 of the main text) yields the exponents  $\frac{\beta'}{\nu}$  and  $\frac{\gamma'}{\nu}$  at those points. The relations between these exponents and the corresponding site-percolation exponents are then verified using Eq. (1) of the main text.

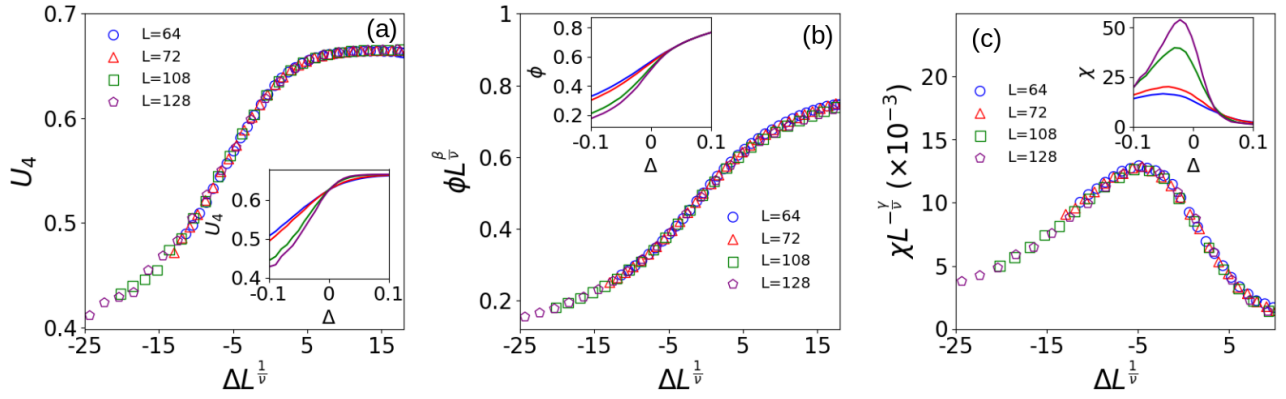


FIG. 9: Critical point IV.  $(p_c, \omega_c) = (0.235, 0.020)$ : (a)  $U_4$ , (b)  $\phi L^{\frac{\beta}{\nu}}$  and (c)  $\chi L^{-\frac{\gamma}{\nu}}$  as a function of  $\Delta L^{\frac{1}{\nu}}$ . The best collapse is obtained for  $\frac{1}{\nu} = 1.43$ ,  $\frac{\beta}{\nu} = 0.140$ ,  $\frac{\gamma}{\nu} = 1.72$ . The inset shows raw data,  $U_4, \phi, \chi$  vs.  $\Delta$ .

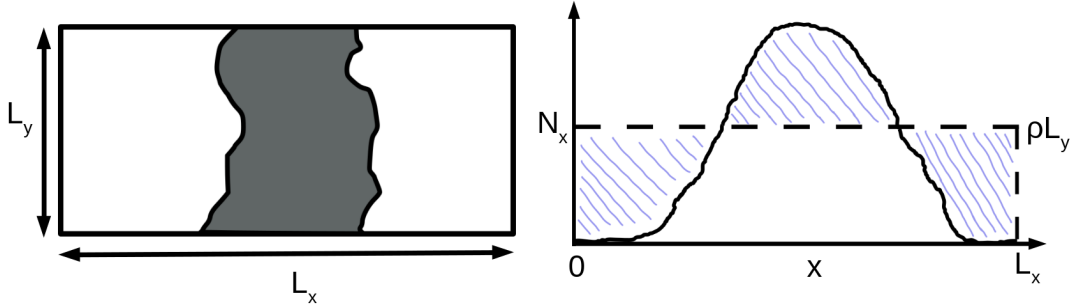


FIG. 10: Schematic configuration of a phase-separated state on a rectangular lattice ( $L_x = 2L_y$ ). (b) The order parameter  $\phi'$  of the system measures how different is  $N_x$  from its mean  $\rho L_y$  in an absolute sense (the shaded area). Here  $N_x$  counts the total number of particles at all the lattice sites  $\mathbf{i} \equiv (x, y)$  which have same  $x$ -coordinate.

- 
- [1] K. Binder, D. W. Heermann, *Monte Carlo Simulation in Statistical Physics* (5th Ed.) Springer Berlin, Heidelberg, 2010.  
 [2] K. Binder, *Phys. Rev. Lett.* **47**, 693 (1981),  
 [3] C. G. Ray, I Mukherjee, P. K. Mohanty, *arXiv:2307.03216*